Carpathian Journal of Earth and Environmental Sciences, April 2010, Vol. 5, No. 1, p. 67 - 82

FORMATION OF A STRATIFORM Zn–Pb-Ag SEDEX DEPOSIT - NUMERICAL SIMULATION

Monica RADULESCU
Universitatea din Petrosani,Geology Department 20 Universitatii street, 332006, Petrosani, Romania
Email: mradulescu@craworld.com

Abstract: This research presents a numerical simulation of the regional scale hydrothermal fluid flow over an E-W geological profile in the Northern Lawn Hill Platform, Australia, at 1575 Ma. The modeling work assesses favorable hydrological scenarios for the formation of stratiform Zn–Pb-Ag SEDEX deposits by buoyancy driven free convection of hydrothermal fluids. Based on recent geological mapping and stratigraphic interpretation, our conceptual model depicts the stratigraphy in the area at the time of mineralization at a finer resolution than previous simulations in the area. The stratigraphic sequence consists of three cycles of clastic and carbonate basin fills, cut by several major syn-sedimentary faults. FEFLOW, a 3D finite element code, is used to simulate fluid flow and coupled heat transfer. Based on a two dimensional simulation, the authors aim to gain insight into the regional groundwater circulation and heat redistribution, discharge at the surface by conduits of faults, and the impact of fluid flow on the mineral precipitation in diagenetic aquifers and deposition on the sea-floor at the vents of discharging faults. The evolution of the hydrothermal system is simulated based on the key hydraulic parameters controlling the paleo fluid flow pattern and heat transport. Numerical simulations indicated the relationship between faults and aquifer sequences as being a major factor controlling buoyancy driven convection. A sensitivity analysis performed for different scenarios by varying relationships between aquifers and syn-sedimentary faults offers a better understanding of the hydrogeological constraints on the genesis of major SEDEX deposits. The purpose of the present study was to target prospective Zn–Pb deposits in the Northern Lawn Hill platform, the Mt. Isa basin by buoyancy driven fluid flow and heat transport.

Key words: numerical modeling, hydrothermal, Isa, Lawn Hill, SEDEX.

1. INTRODUCTION

Sedimentary exhalative (SEDEX) deposits are attractive mineral resources because they account for more than 50% of the world's reserves for zinc, lead and silver (Goodfellow et al. 1993). SEDEX deposits represent the result of paleohydrothermal fluid flow similar to modern sedimentary brines circulation in large-scale hydrothermal systems. Understanding the genesis of this type of sediment-hosted deposits is essential for predicting the location of such deposits (Neacsu et al. 2009, Plotinskaya et al. 2009). Five of the largest SEDEX deposits, including Mount Isa, Hilton, George Fisher, Century and HYC are situated in the northern part of Australia. Early studies (Solomon & Heinrich 1992) suggested that stratiform Pb and Zn ores in Northern Australia were formed by convection of brines in the sedimentary basin and the faulted basement, where the fluid flow was thermally driven by heat from the granitic intrusions.

Mount Isa, a well documented mineralized district (Southgate 2004) (Fig. 1) is one of many Australian Proterozoic terrains with a complex history of sedimentation, magmatism, tectonism, metamorphism and mineralization. Carbonate and quartzite units and numerous unconformities indicate an oscillating sag phase basin setting (Betts & Lister 2002). The volcanic fill, as part of an older rift phase, is a possible source for leached metals and mixed clastics. The Mt. Isa deposits consist of 25 stacked ore bodies over 1 km thickness, hosted by a 1 km thick fill of black dolomitic shale deposited within a second order basin 25 km long created by wrench faulting. The deposits were formed during discrete, episodic events at different

times early in the history of the basin and during basin closure (Southgate et al. 2000a), as a result of fluid migration pulses enabling hydrothermal replacement processes in the subsurface or precipitation at the surface, on the basin floor. With all of the significant Pb-Zn-Ag deposits at the Mt. Isa Basin being younger (1575 Ma) than the rifting event (1710 Ma), the pre-existing extensional structures represented an essential part of the hydrothermal system for the circulation of mineralizing fluids (Betts 2000). The mineralization occurred around 1575 Ma during the post rift and shallow–water sag phase of rift development when shallow water sandstone-carbonate sedimentation predominated. Therefore, fluid flow and heat transport are crucial processes for understanding the genesis of the Mt. Isa SEDEX mineralization.

Computer simulations have been widely used to solve heat transfer and fluid flow problems in hydrothermal systems, including systems responsible for the formation of SEDEX deposits (Hobbs et al. 2000, Simms & Garven 2004, Yang et al. 2004 a, b).

Previous investigations in the Lawn Hill Platform, as part of the Mt. Isa basin, addressed a N-S vertical cross section, termed profile P1, from the Murphy Inlier in the north to the Cambrian outcrop in the south, between $17^0$30' to $19^0$00' along $138^0$30' longitude (Fig. 1). The numerical simulations performed for this profile took into account buoyancy driven fluid flow (Yang et al. 2006) and tectonic deformation (Zhang et al. 2006) and described the most favorable hydrogeological conditions for the formation of a Century- style ore body. These initial attempts provided interesting results, although based on simplified constraints. The same computational code was used by Koziy (2004) who simulated buoyancy driven fluid flow and heat transport along an E-W transect, termed profile P3 (Fig. 1) in the northern Lawn Hill Platform.

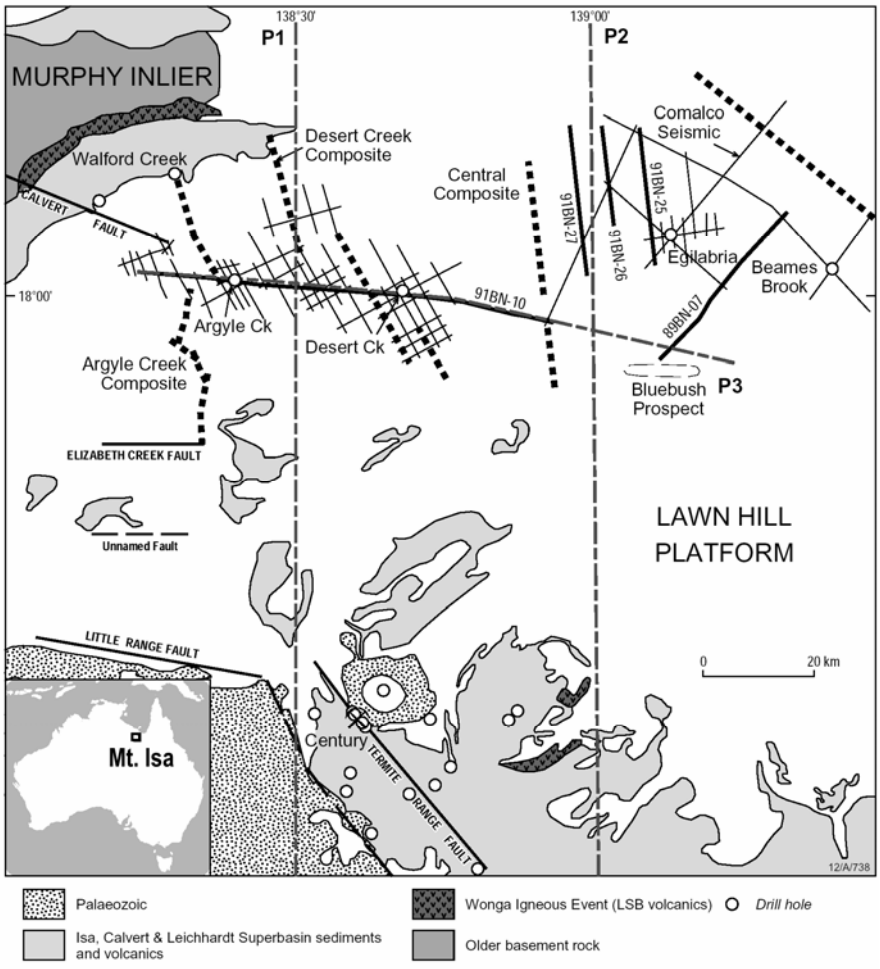

Figure 1. Detailed map of the Lawn Hill platform, with: geological transects P1 and P3, the Comalco seismic grid with 91BN-10, drill holes, Superbasin and Igneous event geology and the major faults (Calvert, Elizabeth Creek, Termite Range and Little Range) (after Blake 1987, McGoldrick and Large 1998, Winefield 1999, Scott & al. 2006).

At that time, besides the used mesh being relatively coarse, the modeling results were numerically unstable due to the limitations of the code (Koziy 2004). In a response to these results, the present study aims for a better stability of the numerical modeling of the hydrothermal system and improvement of the mesh size. The study uses FEFLOW (WASY 2005), a 3-D finite element code modeling coupled fluid flow, mass and heat transport, to simulate buoyancy driven fluid flow and heat transport along the same E-W transect, P3, in the northern Lawn Hill Platform. FEFLOW allows flexible unstructured meshing with transitional mesh density, for a close representation of complex stratigraphy. Meshes were designed with an average of 12000 nodes and 25000 elements, determined according to different configurations tested for the stability of the simulations.

The purpose of the present 2D simulation is to investigate the impact of the regional groundwater circulation at 1575 Ma on the formation of SEDEX deposits in the Northern Lawn Hill platform. The regional scale of the model added additional challenges to the conventional hydrogeological modeling, because smaller-scale features such as faults have to be incorporated in the large-scale system. These faults act as conduits for the hydrothermal fluid flow, enhancing vertical fluid migration or directing the circulation of fluids into horizontal formations, where precipitation of minerals may occur.

The current simulations consider extensive geological information and describe the evolution of a hydrothermal, non–boiling, single–phase fluid flow coupled with heat transport. A sensitivity analysis has also been conducted to assess the influence of varying hydrogeological parameters and hydrostratigraphy on the fluid flow patterns, discharge temperatures and velocities along the regional E-W profile P3. Previous studies (Evans & Raffensperger 1992; Garven 1995a) showed that fluid flow in submarine environments can be driven by buoyancy forces as a result of fluid density gradients, temperature, salinity and pressure. Garven (1995b) showed that for systems where topographic drive is weak, flow due to density-driven convection dominate. For the present study, we do not consider topographic drive, as fluid flow is driven by buoyancy, controlled by variable-density and viscosity of the fluid as a function of temperature. No account was taken for the effects of salinity. Darcy fluid velocities and temperature distributions are the major output parameters. The most favorable conditions for the formation of stratiform Zn-Pb-Ag deposits at 1575 Ma in the Lawn Hill mineral field are determined and exploration target areas are predicted.

2. GEOLOGICAL FRAMEWORK

2.1 Tectonic settings and Superbasin structures

The Mt. Isa Basin in north-west Queensland hosts four giant Zn-Pb±Cu deposits (Mt. Isa, Hilton, George Fisher and Century) and smaller Cu and Zn-Pb deposits. These deposits formed between 1670 to 1575 Ma mainly in carbonaceous and calcareous shales and siltstones.

The Mt. Isa superbasin consists of three tectonic belts (Fig. 2): the Western Fold Belt, the Kalkadoon-Leichhardt Belt and the Eastern Fold Belt (Blake 1987; Jackson et al. 1990). The Western Fold Belt is represented by the Lawn Hill Platform, the Leichhardt River Fault Trough, the Ewen Block and the Myally Shelf (Blake 1987). Most of the Zn-Pb ore mineralizations are hosted in the youngest stratigraphic sequences of the Western succession of the Mt Isa Basin, consisting of carbonate, carbonaceous siltstone and shale formations, known as the McNamara Group on the Lawn Hill Platform and the Mt Isa Group in the Leichhardt River Fault Trough (Fig. 3). Extensive geological and geophysical investigations in the Western Fold Belt (Jackson et al. 2000; Krassay et al. 2000a, b; Page et al. 2000; Southgate, et al. 2000a,b) reiterated that the McNamara Group and Mt Isa Group belong to the Isa Superbasin (Fig. 3).

2.2. Paleobasin geometries for the central and northern Lawn Hill Platform

The timing of the Isa Superbasin deposition occurred from ca. 1670 Ma to ca. 1575 Ma (Krassay et al. 2000b; Page et al. 2000; Southgate et al. 2000a). Based on seismic profiles investigated to the north of the Century Zn-Pb deposit, on the northern Lawn Hill Platform, Scott et al. (2004) showed that at 1575 Ma the Mt. Guide Quartzite and Eastern Creek Volcanics were approximately 20 to 25 km below the Isa Superbasin trap rocks. Polito et al. (2006b) suggested that across the northern and central Lawn Hill Platform, the Calvert Superbasin could have been an aquifer and potential source rock for the Zn-Pb deposits formed at 1575 Ma. At this time, the rocks of Calvert age were buried to depths of 7 to 11 km on the central and northern Lawn Hill Platform.

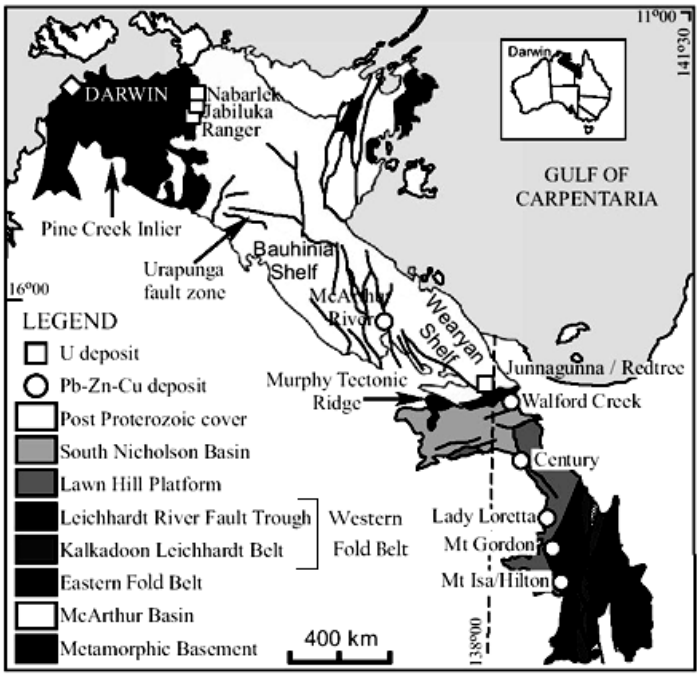

Figure 2 Geological map of the Mt. Isa Basin: the eastern fold belt, the Kalkadoon Leichhardt Belt and the western fold belt (including the Lawn Hill Platform and the Leichhardt River Fault Trough). Also shown on the figure the South Nicholson Basin, McArthur Basin and related U deposits and SEDEX Zn-Pb and Cu deposits (Polito & al, 2006b).

2.3. Sources of metals

The mineral paragenesis research (Polito et al. 2006a) in the Mt. Isa basin outlined regional diagenetic aquifers, represented by deeply buried fluid reservoirs where secondary porosity during burial diagenesis was created by the destruction of unstable mineral grains in contact with basinal fluids already resident in the associated pore spaces. The fertile brines represent a leaching product of the metals present in these unstable grains. As a result, reliable information about the metal source for the Zn-Pb and Cu deposits is obtained through the identification of diagenetic aquifers spatially and temporally associated with volcanic units. The clastic sediments in the Leichhardt and Calvert Superbasins are related to two diagenetic events: (1) early diagenesis during shallow burial at low temperatures; and (2) peak diagenesis at depths where high temperatures favored the solubility of siliciclastic and carbonate grains and precipitation of other stable phases. In the Mt. Isa Basin, the Mt. Guide and Lena Quartzites lithologies, belonging to the lower Leichhardt Superbasin, present the most important diagenetic alteration and fluid to rock ratios during peak diagenesis. The Mt. Guide and Lena Quartzites occur adjacent to or within the mafic Eastern Creek Volcanics and may be interpreted as diagenetic, metal-bearing aquifers (Wyborn 1987). However, according to Polito et al. (2006b), at 1575 Ma the Leichhardt Superbasin was buried to a depth that precludes it from being a potential fluid and metal source. Petrological and geochemical evidences from the Leichhardt River Fault Trough show that the Calvert Superbasin strata had the physical, mineralogical and diagenetic potential to be a source aquifer for metals.

Diagenetic aquitards may occur when burial diagenesis resulted in the early occlusion of primary permeability in some facies (Hiatt et al. 2001, Damian et al. 2009). The sandstones and carbonates lithologies belonging to the upper Leichhardt, the Calvert and the Isa Superbasins were sealed early by quartz overgrowths during a diagenetic event and present low fluid-rock ratios. As a result, these lithologies, reaching depths of 6 to 11 km in the Lawn Hill Platform, are interpreted as being seals or diagenetic aquitards.

2.4. Fluid temperatures

Illite crystallinity data and chlorite chemical compositions indicate that basinal brines in the Leichhardt Superbasin were at temperatures ranging between 150 and 230ºC. Maturation of organic matter in the Lawn Hill Platform indicates that temperatures were variable, with the lowest values recorded close to the Murphy Inlier and the highest values in supersequence boundaries and proximal to the active fault systems (Polito et al. 2006b).

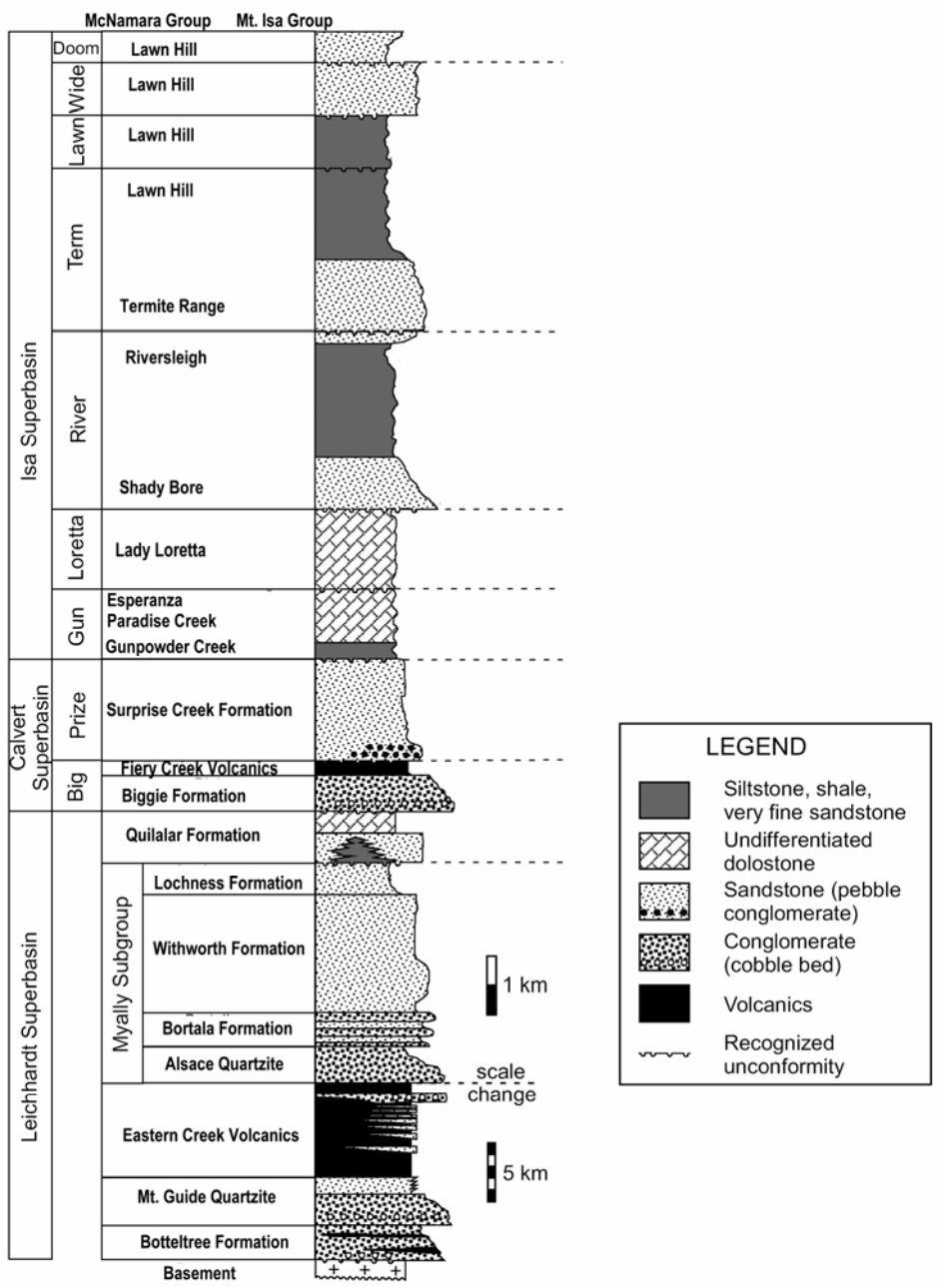

Figure 3 Stratigraphic column for the Western succession of the Mt Isa Basin subdivided into the Leichhardt, Calvert and Isa Superbasins (after Jackson & al. 2000, Scott & al. 2004).

2.5. Timing of hydrothermal fluid expulsion

Stratigraphic sequences correlated with palaeomagnetism datasets (Idnurm 2000) show that basinal fluid-flow events that generated the sediment-hosted mineralization were initiated by major tectonic events with intraplate stress variations (Southgate et al. 2000a). Pb/Pb isotopes model ages indicate the Lawn Hill and other syn - to late orogenic veins were formed in the period of 1575-1500 Ma (Carr et al. 1996), as a result of interplate tectonic events. This assumption is supported by the theory of Garven & Freeze (1984), where brines were driven during the Isan orogeny. The Isan Orogeny probably initiated fluid migration from the Calvert and Isa Superbasin aquifers (Polito et al. 2006b). Consequently, the present research will investigate the circulation of a homogeneous, saline basin-derived fluid within the Lawn Hill Platform of initial meteoric origin, at 1575 Ma, during the initial stages of closure and inversion of the Isa Superbasin. The ore bearing brine water is thought to be initially derived from meteoric water infiltrated during the incipient phase of basin rifting, which leached ore forming components from source

rocks during its repeatedly circulation as groundwater (Polito et al. 2006a).

3. HYDROTHERMAL FLUID FLOW MODELING

3.1. Method

The present hydrothermal modeling is carried out using FEFLOW 5.1, developed by WASY (2005). FEFLOW is a 3D finite element code capable of modeling of density-dependent fluid flow and mass and heat transport (Diersch 1992, 1993). The flow modeling is based on mass conservation in porous media. The heat transport is based on advection-conduction and free convection of heat.

The solution of the governing differential equations and boundary conditions is achieved using an implicit adaptive time stepping scheme (adaptive error controlled time steps), with variable time steps (Diersch 2005).

FEFLOW uses for mesh generation Triangle, a specialized code for creating two-dimensional finite element meshes (Shewchuk 1996, 2002). The mesh generator supports the dimensions and complex geology of the model, allowing the realistic representation of a large scale area discretized into triangular elements. The triangular finite elements meshes were generated based on prior so called "superelements", which represent the conceptualized hydrostratigraphic frame.

For the present model the frame used to build the mesh on described the system at 1575 Ma and remained unchanged during the simulation. A limitation of the code is the lack of ability to modify the structure of the superelements during the simulation. Consequently, the resulting model was "geometrically fixed", which means that no tectonic and hydrostratigraphic evolution was accommodated during the simulations.

The changing hydraulic conditions within the upper aquifer upon precipitation of minerals were simulated by assigning a variable hydraulic conductivity, decreasing linearly with one order of magnitude for each one million years as well as a variable porosity. The moderate decrease was attributed to simulate the gradual loss of porosity during diagenetic processes. No changes to other geological structures or hydraulic parameters within the remaining formations in the model were performed.

The postprocessing of simulated data evaluated the fluid flux, heat flux analysis, Darcy flow velocity, distribution of hydraulic head, mass and generated graphical output for fluid flow and heat transport.

3.2. Paleo – hydrostratigraphic model conceptualization

The Lawn Hill platform is a well documented area in terms of tectonic settings, basin geometry, stratigraphy and sedimentology (Leaman 1998; Bull 1998; Southgate et al. 2000a; Scott et al. 2004). Recent petrographical, geochemical, and isotopic investigations addressed the likely source of mineralization fluids by delineation of aquifers, reservoirs, cap seals and source rocks for the metals (Large et al. 1998, 2000, 2001, Cooke et al. 2000, Golding et al. 2006, Polito et al. 2006b).

The E-W profile, termed P3, extends from $138^0$15' to $139^0$00' along latitude 18^0 S (Fig. 1). The construction of the present day profile relied on stratigraphic features obtained from the seismic line 90BN-10 (Fig. 4). The model was reconstructed at ~1575 Ma (Scott et al. 2004) (Fig. 5).

The conceptual paleo-hydrostratigraphic frame used for the simulations was based on the stratigraphic and structural profile P3 at ~1575 Ma and previous modeling work (Koziy 2004). Key elements of ore deposit formation, such as metal source, basinal hydrothermal fluid reservoirs, migration patterns, faults and the basin geometry within a comprehensive time-space perspective were incorporated in the conceptual model.

Petrographic and geochemical investigation in the Mt. Isa and McArthur basins (Polito et al. 2006b) suggested the presence of two sub-horizontal aquifers in the stratigraphic sequence of the P3 profile: the upper aquifer formed by sandstones and volcaniclastics as part of the Big Supersequence at the base of the Calvert Superbasin and presumably, the lower aquifer formed by sandstones and conglomerates as part of the Mt. Guide and Lena Quartzite at the base of the Leichhardt Superbasin (Fig. 3). The aquifers facilitate the lateral fluid flow in the basin and the upward flow of the heated fluids from the basement to the potential source rocks. The presence of the top sedimentary layer, with very low hydraulic conductivity, acts like a seal for faults not reaching the surface.

Four primary, syn-sedimentary, basement rooted faults intersecting profile P3 were active during the period of time 1640-1575 Ma, according to Scott et al. (2004). Faults penetrating the basement act as enhanced fluid flow conduits and account for more vigorous flow through the two interconnected aquifers. Secondary faults penetrating into the upper aquifer and connecting with primary faults may play an important role in the

discharge-recharge pattern of the fluid flow.

The 2D conceptual model is illustrated in Figure 6**.** The model extends 120 km horizontally and 33 km vertically and consists of seven hydrostratigraphic units, presented in Table 1, along with the hydraulic properties of the model, based on previous studies in this area (Koziy 2004; Yang et al. 2006).

The geometry of the model was transformed into a complex unstructured mesh that matches closely the hydrostratigraphic setting, while taking into account requirements as element size and element angles in order to avoid further numerical oscillations during the simulation. The superelements in the mesh correspond to the hydrostratigraphic units in figure 6. Figure 7 presents an outline of the model, with two dimensional finite elements mesh generated over the superelements.

The hydraulic conductivities were defined according to the fluid conditions at a reference temperature and pressure and they are anisotropic throughout the model, with a factor of Kx/Kz=100, due to the vertical compaction of the geological strata (Raffensperger & Garven 1995). The faults are assumed to be permeable, homogenous and isotropic for all the hydraulic parameters.

Hydraulic conductivities were constrained by mineral paragenesis and geochemical information about the lithology in the Leichhardt, Calvert and Isa Superbasins (Polito et al. 2006b; Golding et al. 2006).

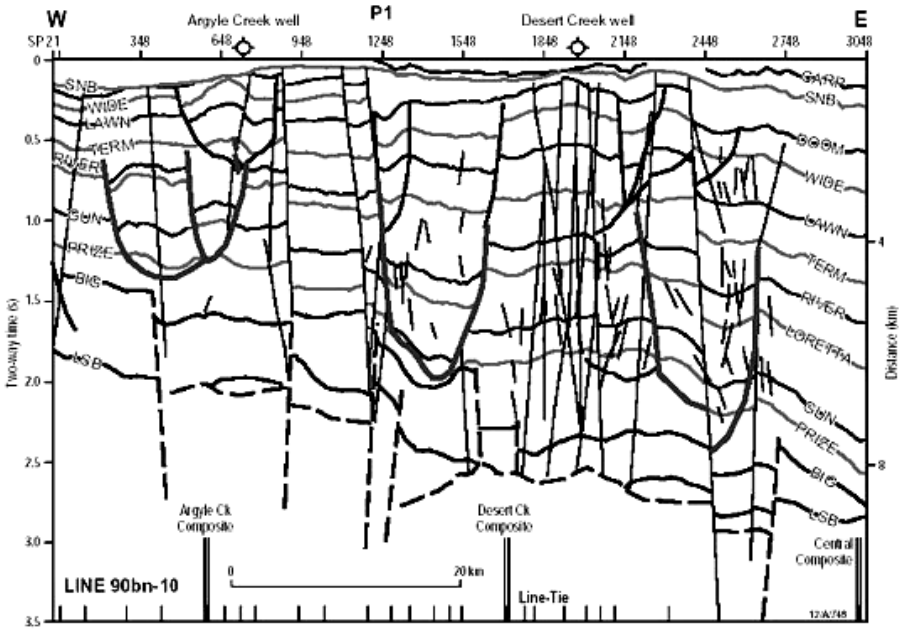

Figure 4 Seismic line 90BN-10 coincident with the western 75km of profile P3 used to constrain the geometry of the Isa Superbasin stratigraphy (after Bradshaw & Scott 1999, Scott et al. 2004).

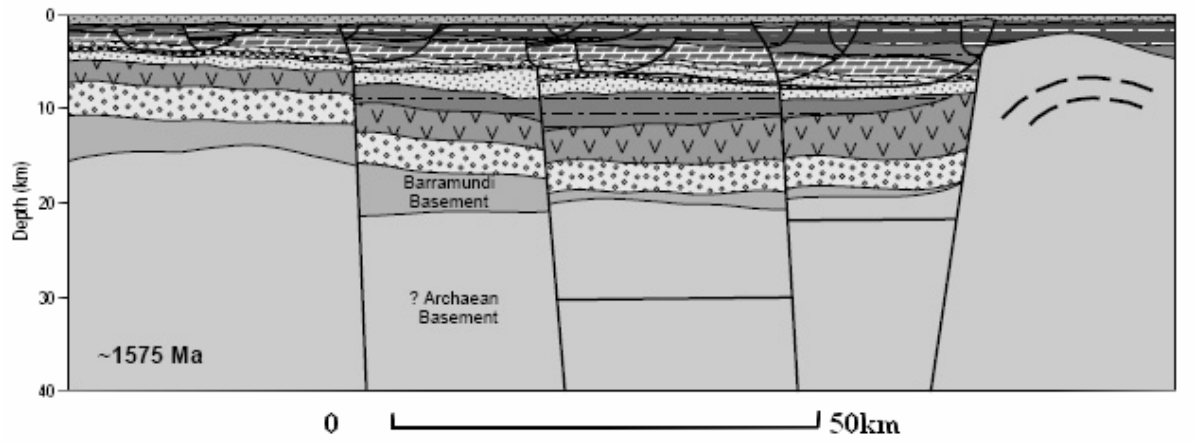

Figure 5 Reconstruction of the model at ~ 1575 Ma. (Scott & al. 2004).

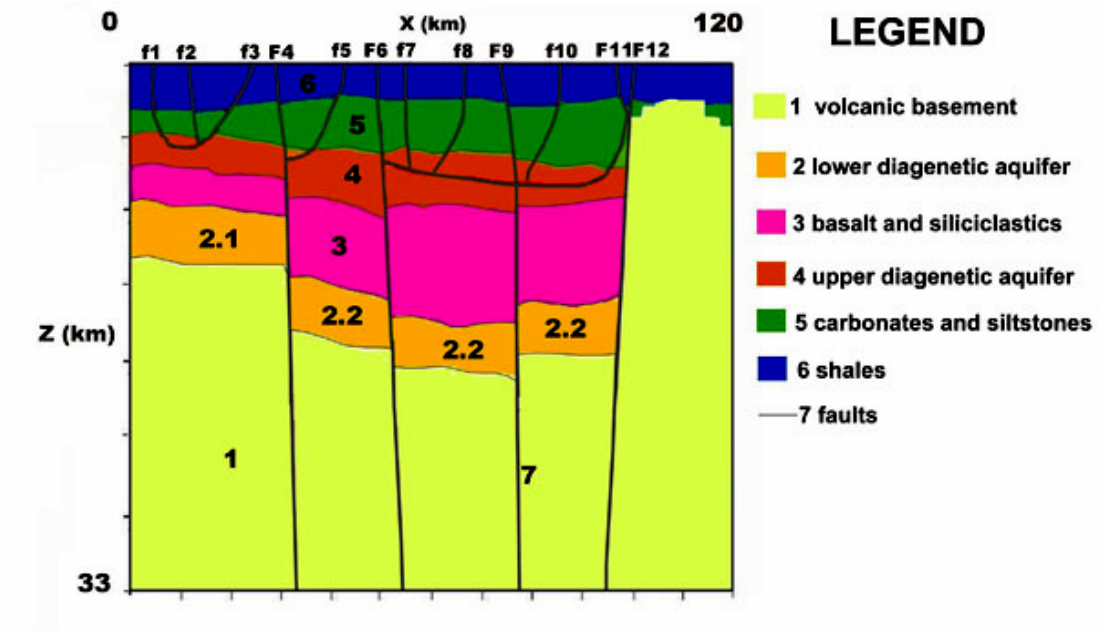

Figure 6 2D hydrostratigraphic conceptual model, vertical exaggeration 3:1. The hydrostratigraphic units 1-7 were over imposed as superelements during the generation of the finite elements mesh. Note: The screenshots of temperature distribution superimposed over the fluid velocity from figures 8,9 and 10 preserve the same vertical exaggeration, 3:1.

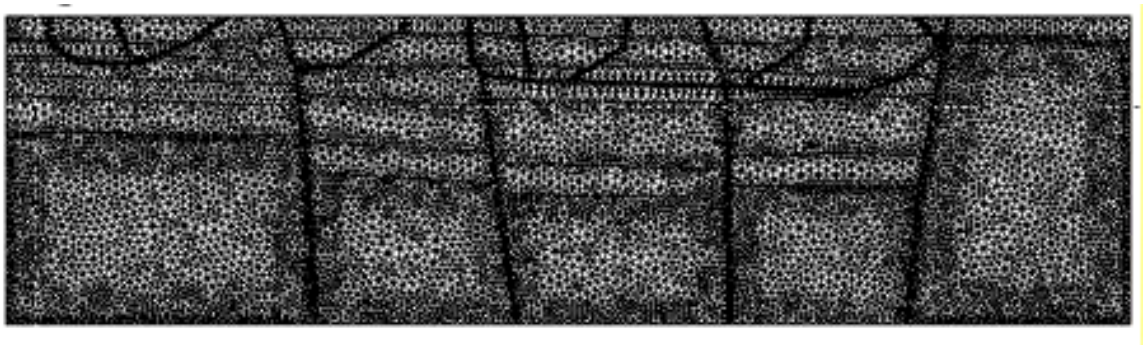

Figure 7 Outline of the hydrostratigraphic model, with finite elements mesh, 1:1. The vertical exaggeration was not applied for this figure in order to preserve the proportions of the finite elements.

Table 1 Hydrostratigraphic model

Rock unit	Stratigraphy of the rock unit		Hydraulic conductivity (K_x) (m/s)	Porosity [%]
1	Basement of granite: old Archaean crust, Cliffdale volcanics, Nicholson granite and/or Murphy metamorphics and Barramundi basement		5.484×10^{-13}	10
2	Lower aquifer of siliciclastics, coarse grained sandstones and conglomerates: Mt. Guide quartzite, Westmoreland Conglomerate and Wire Creek formation from Leichhardt Superbasin	2.1	5.484×10^{-9}	20
		2.2	5.484×10^{-11}	20
3	Intermediate layer of basalt and fine grained siliciclastics: Eastern Creek volcanics and Buddawadda basalt, Leichhardt Superbasin		5.484×10^{-11}	10
4	Upper aquifer of sandstones, conglomerates and volcaniclastics: Bigie and Fiery Creek and upper Peters Creek Volcanics, Calvert Superbasin		5.484×10^{-7}	30
5	Carbonates: Lady Loretta Formation, Loretta Supersequence, Isa Superbasin		5.484×10^{-9}	20
6	Top sedimentary layer: Lawn formation		5.484×10^{-11}	10
7	Faults		5.484×10^{-7}	30

The volcanic and metamorphic basement in the model was assigned a hydraulic conductivity in the range of 10^{-13} m/s, at 18-33 km of depth. The upper aquifer was assigned a hydraulic conductivity of $\approx 10^{-7}$ m/s. The two sections of the lower aquifer were assigned hydraulic conductivity 2 to 4 orders of magnitude lower than the higher aquifer, due to increased depth. For the present modeling effort, hydraulic conductivity proved to be a crucial parameter for the two aquifers assumed to be responsible for: a) the circulation of the ore fluid in the hydrothermal system and b) for the carbonate and siltstone formation, the confining unit behaving as an aquitard.

Porosities of the rock units were assigned based on previously published literature (Hiatt & Kyser 2000; Pittman 1979), from 10 to 20%. Faults were assigned porosities of 30%, a value based on previous similar hydromodeling studies in the area (Yang et al. 2006).

Regional-scale longitudinal dispersivity of 1000 m and transverse dispersivity of 100 are assigned for the rock units. Dispersivities are chosen two orders of magnitude lower for the faults, respectively 10 and 1 m. These values are reasonable for the scale of the present model (Neuman 1990; Gelhar et al. 1992; Xu & Eckstein 1995). Further testing of the model was performed to verify the accuracy of the simulation for finer discretization of the mesh and smaller dispersivities, as in the case of the faults. The Peclet number proved to be small enough to achieve accurate results.

Previous studies in the area utilized a value of 2.5 $Jm^{-1}s^{-1}\ {}^{0}C^{-1}$ for the thermal conductivity, calculated from porosity and thermal conductivities of the mineral constituents and of the fluids (Yang et al. 2006). This value was used for all of the rock units.

As conduits for fluid flow, tectonically active faults during the mineralization event have been assigned a hydraulic conductivity which is generally two orders of magnitude higher than the conductivity of the upper aquifer, whereas the inactive faults were simulated by assigning a hydraulic conductivity consistent with each of the geological formations they penetrate. Consequently, the effect of changing the hydraulic conductivities along the faults is investigated in a further sensitivity analysis.

The initial conditions for the transient runs were based on the results of a steady-state simulation of hydraulic heads and temperature.

The lower boundary is assumed to be impermeable to fluid flow and isothermal at 720^0 C. The assigned temperature is justified by the thermal maturation studies of Glickson et al. (2006), which revealed a moderate geothermal gradient of 22-24^0C/km for the northern Lawn Hill Platform. Previous studies (Andrews 1998; Krassay et al. 2000b; Page et al. 2000) showed that marine conditions persisted over 1640 to 1595Ma in the Lawn Hill platform, during the deposition of the upper Isa Superbasin. Accordingly, the upper boundary of the model, representing the sea floor, is isothermal and permeable to fluid flow, such as the sea water can recharge the basin and hydrothermal fluids can discharge to the sea floor. The upper boundary is maintained at a fixed temperature of 10^0C, characteristic for a shallow seafloor bottom (Simms & Garven 2004). The side boundaries are assumed to be impermeable to fluid flow and adiabatic to heat transfer. The horizontal extent of the model and the distance between the side boundaries are large enough not to have a significant influence on the fluid flow inside the system.

3.3 Description of model case

Simulations were performed for one structural case: major faults penetrate the entire basement and all the faults reach the model surface of the domain. Various scenarios were performed to assess the effects of faults open (active) and closed (inactive) and presence of diagenetic aquifers in the system. The faults are removed from the system by lowering their hydraulic conductivity to the values similar to those of host rocks, so that they do not act as fluid conducts. These scenarios are: Scenario a) active minor faults and inactive major faults; b) active major faults and inactive minor faults; and c) all faults active. Except for the hydraulic conductivities and porosities of the faults, all the other physical parameters are kept the same as shown in Table 1.

According to Goodfellow et al. (1993), fluid-rock reactions within SEDEX hydrothermal systems take place in zones where brines are generated, that is in the diagenetic aquifers where fluids reside, and in discharging faults along which fluids circulate to the seafloor.

Two assumptions of the present model are that the prospective Pb-Zn SEDEX deposits in the Lawn Hill platform were formed: a) below the basin floor during basin inversion by syn-genetic replacement of organic-rich lithologies by fluids emanating from the faults and b) by mineral precipitation at the outlets of the discharging faults on the sea-floor. These assumptions are in agreement with previous findings related to the formation of the Century deposit in the vicinity of the Termite Range fault (Broadbent et al. 1998).

Southgate et al. (2000a) showed that mineralizing events were associated with tectonically active periods, when the faults were active. Consequently, the simulations were run for a period of 1.4 million years, corresponding to a hydrothermal fluid pulse during the Isan orogeny.

The assumptions associated with buoyancy driven free convective models were: a) hydrothermal fluids recharge the basin via the faults and flow predominantly through the sandstone and volcaniclastic aquifers and b) the brines have the potential to leach metals from the aquifers.

The model addressed the following questions:

- Which were the flow patterns during the Isan orogeny, when fluids within the system circulated through metal bearing source rocks or sediments?
- Which was the influence of major, basement-rooted faults and minor faults on the fluid flow and heat transport throughout the basin, described as a relationship between flow of brines and thermal pattern?
- Where the faults acted as discharge conduits, were there any favorable conditions upon fluid exhalation for precipitation of minerals?
- Where the fluids resided in the diagenetic aquifers, were the temperatures in the basin favorable to mineral precipitation and forming of ore deposits?

4. MODELING RESULTS

In figures 8, 9 and 10, depicting the heat distribution and hydrothermal fluids circulation patterns, the flowing paths along the faults and within the aquifers are represented by arrows, where the relative sizes of the arrow suggest the relative velocities of the fluid.

In the case of faults reach both upper and lower boundaries of the model, major observations are as follows:

a) When minor faults are active and major faults sealed, fluid flow occurs mainly within the upper aquifer and along the faults penetrating it. With major faults inactive, the flow is insignificant in the basement and very low in the lower diagenetic aquifer and the overlying basalt and fine grained siliciclastics formation. Consequently, the temperature variation at greater depths is controlled only by thermal conduction (Figure 8). In the meantime, cold fluid is actively circulated downwards from the surface into the upper aquifer (0.95-1.85 m/year), lowering the temperature within it to 50-70^{0}C and accordingly the temperature along the discharging faults. The upwelling fluids on f1, f5 and f8 reach the vents at velocities of 1.3-5.6 m/year and temperatures of 24 to 43^{0}C. The most vigorous discharge takes place along f5, with v_{max}= 5.6 m/year at 43^{0}C.

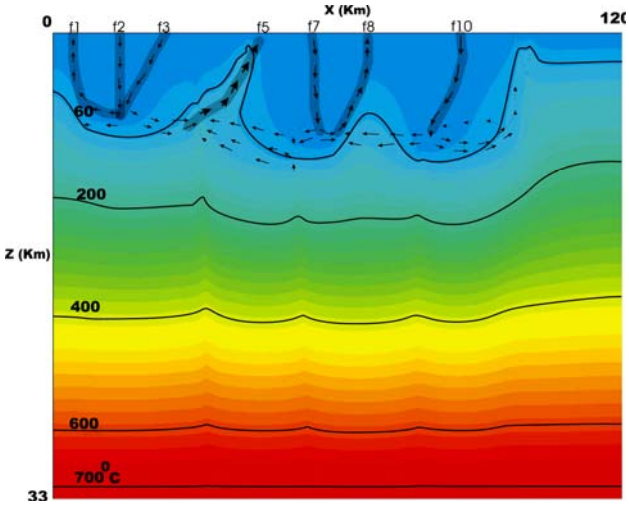

Figure 8 Temperature distribution superimposed over the fluid velocity for faults reaching both upper and lower boundaries of the model, minor faults active. Cold fluid circulated downwards from the surface into the upper aquifer at 0.95 to 1.85 m/year lower the temperature at 50 to 70^{0}C. Discharge temperatures at f1, f5 and f8 vary between 24-43^{0}C, for v = 1.3-5.6 m/year. f5 is discharging at v_{max} = 5.6 m/year and 43^{0}C.

b) Discharge temperatures on the sea-floor vents become higher (between 127-180^{0}C) when major faults are active and minor faults are closed, as the fluid flow transports the heat from the hot basement to the surface (Fig. 9). Fluid temperatures in the upper aquifer and above it are increased, from 60^{0}C on the left side to 400^{0}C in the central section. Provided suitable trap rocks, the accumulation of ore by precipitation of sulphides is likely to occur in the central section of the model, between F4-F6 and F9-F12. Major faults F4 and F12 are recharging during the first 0.75 Ma, reversing to the state of discharge conduits for fluids from the basement and from adjacent porous formations onto the sea floor for the next 0.65 Ma of the simulation. At 1.4 Ma, the Darcy velocity of the fluid at the vent of F12 is 4.75 m/year for a temperature of 133^{0}C, while the maxim discharge velocity in the system is reached at F4, 5.82 m/year at 136^{0}C (Fig. 9). The higher density of colder fluid circulated from the surface along faults F 6 and F9 suppresses the circulation of upwelling, lower densities hot fluids from the basement. As a result, F6 and F9 change polarity within the upper aquifer, a phenomenon which generates a convection cell between F4-F6. A further quantitative analysis will be performed to test the possibility of a stratiform ore accumulation by discharge of

hydrothermal fluids at the vents of F4 and F12.

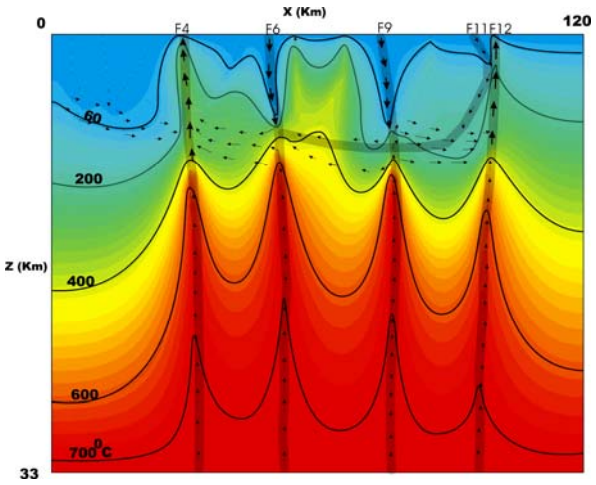

Figure 9 Temperature distribution superimposed over the fluid velocity: faults reach both upper and lower boundaries of the model, major faults active. Discharge temperatures vary between 127-180^{0}C. Provided suitable trap rocks, the accumulation of ore by precipitation of sulphides is likely to occur in the central section of the model, between F4-F6 and F9-F12. For F12, v = 4.75m/year at 133^{0}C. For F 4, v_{max} = 5.82 m/year at 136^{0}C. A quantitative analysis showed a potential Zn accumulation, after 25% precipitation upon exhalation of the hydrothermal fluid, of approximately 16 million tones in the vicinity of F4 and F12 vents.

c) When all faults become tectonically active, open to fluid flow, enhanced fluid circulation occurs from the basement, within the upper aquifer and along the faults reaching it (Fig. 10). Greater hydraulic conductivity contrast between faults and adjacent rocks delivers more recharge into faults. Major faults from the basement allow penetration of hot fluids into the upper aquifer, while recharge with cold water occurs from the sea-floor along most of the faults: f2, f3, f5, f7, f8, f9 and f10. Significant recharge occurs by f5, f8 and f10, at Darcy velocities of 19.52-25.12 m/year. As a result of the enhanced recharge with cold water, heat transport from the basement is suppressed by the cold water influx and temperatures in the upper aquifer range from 40 to 180^{0}C. The most favorable section for replacement style mineral accumulation is between major faults F6-F4, where temperatures in the range of 80-180^{0}C are compatible with previous findings in the area (Polito et al. 2006b). However, Darcy velocity in the mentioned section is lower than other velocities within the upper aquifer, suggesting the potential accumulation of low-grade ore. Discharge temperatures at the vents are between 23-42^{0}C, approximately in the same range as in the case where only minor faults were active. The maximum Darcy velocity in the system is reached for F6, which acts as the main discharge conduit, with a velocity of 35.23m/year and 42^{0}C at the vent.

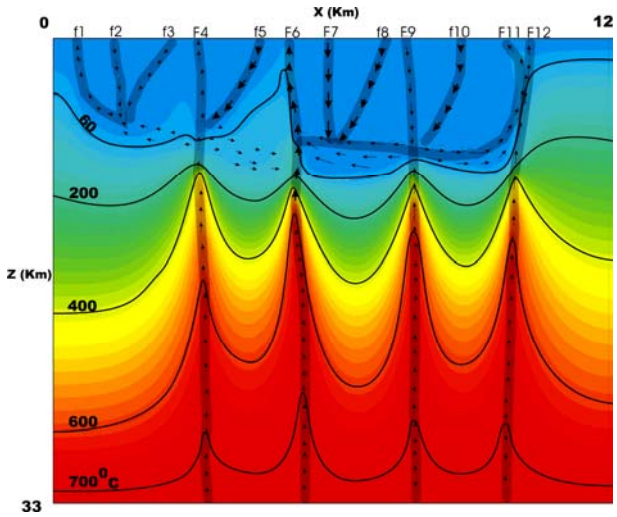

Figure 10 Temperature distribution superimposed over the fluid velocity: faults reach both upper and lower boundaries of the model, all faults active. Significant heat transport from the basement is suppressed by the cold water influx and temperatures in the upper aquifer range from 40 to 180^{0}C. The most favorable section for replacement style mineral accumulation occurs between major faults F6-F4. Discharge temperatures at the vents are 23-42^{0}C . F6 is discharging at v_{max} = 35.23 m/year and 42^{0}C.

5. DISCUSSION OF RESULTS

5.1. Fluid flow pattern, heat distribution and prospective mineral accumulations

Throughout all the simulated scenarios, the uplifted basement block on the western side of the model creates a sharp contrast of hydraulic properties between the upper aquifer and basement, separated by F12, with direct repercussion on the flow pattern and heat distribution. Cold recharging fluids from the sea-floor have a significant influence on lowering the temperatures within the upper aquifer, as it can be observed from figures 8, 9 and 10.

Discharge temperatures at the vents between 45 to 60^{0}C are not favorable for the accumulation of any significant Zn-Pb deposit, however, this range may be characteristic for low-grade exhalation type ores of Mn and Fe (HYC, Large et al. 2000). Discharge temperatures of 100 to 300^{0}C are favorable for the accumulation of Zn-Pb SEDEX deposits, as described by Goodfellow et al. (1993) and Cooke et al. (2000). Consequently, the situations where the temperatures at the vents of the

discharging faults were within the above mentioned range were quantitatively investigated to test the possibility of the formation of a stratiform SEDEX deposit.

Tectonically active minor faults do not enable the accumulation of a SEDEX type ore-deposit as temperatures at the vents on the sea-floor are below 43^0C for corresponding discharge velocities in the range of $3.7x10^{-5}$ to 5.6 m/year.

Tectonically active major faults which penetrate the top sedimentary layer produce a significant volume of fluid discharge on the sea-floor, at temperatures from 110 to 180^0C. This discharge temperature range represents a favorable scenario for the potential accumulation of a SEDEX Zn-Pb-Ag ore deposit (Goodfellow et al. 1993; Cooke et al. 2000). The temperatures within the upper diagenetic aquifer are in agreement with mineral and fluid inclusions described by Polito el al. (2006b). With the deeper diagenetic aquifer of siliciclastics, coarse grained sandstones and conglomerates as a potential source for metal-bearing fluids, higher discharge temperatures associated with significant fluid velocities at the vents of the faults enable the potential accumulation of a SEDEX type deposit.

For tectonically active major faults rooted in the basement and reaching the surface (scenario b outlined above) the discharge volume for F4 is of about 498 m^2/year (per meter of fault strike). Assuming a fault length of 2000 m and the discharging fluids carrying about 100 ppm Zn (Cooke & al. 2000), then the accumulated metal over a discharge period of 0.65 Ma years, provided 25% of the zinc carried by the fluid is precipitated upon exhalation, is 16 million tones of Zn metal, a value consistent with an already defined ore deposit at Century, of 14 million tones. At comparable velocities and depth of penetration within the upper aquifer, results at the vents of F12 are similar to the ones achieved for F4.

With all faults tectonically active and breaching the top impermeable layer, regardless the major faults extent at greater depths, venting temperatures as well as temperatures within the upper aquifer are to low to enable a Pb-Zn stratiform accumulation on the sea-floor at the vents of the faults or by mineral replacement within the trap rocks.

6. CONCLUSIONS

Fluid and heat transport over P3, an E-W geologic profile in the northern Lawn Hill Platform of Australia, was simulated by using the finite element code FEFLOW.

The research was structured on two levels: Firstly, we investigated the influence of varying hydrogeological parameters and structural features on the fluid flow patterns, heat distribution, discharge temperatures and Darcy velocities in the system.

The simulations showed that fluid flow and heat transport as well as the discharge/recharge pattern at the vents of the faults on the sea-floor are controlled by the following factors:

- Structural features of the models: numerical modeling showed that the structure and hydraulic properties of the faults played a major role in the fluid flow pattern and heat transport. The two aquifers interconnected by faults play different roles in developing the flow and heat pattern, due to the reduced hydraulic conductivities of the lower aquifer. Hot fluids coming from the basement heat up the aquifers, with the most active flow occurring in the upper aquifer. Higher temperatures in the coarse grained siliciclastics of the lower aquifer represent a favorable scenario for the leaching of minerals, followed by transport of the enriched brines along the faults. In the upper aquifer, the marine water recharging the system along certain faults mixes with the hot fluids coming from the granite basement and, depending on the distribution of active faults, fluid flow patterns become more complex. As a result of the temperature gradients, structural features (lower aquifer slightly deepening towards the east, fault spacing, aquifer thickness) and hydraulic parameters, convective cells form within and above the upper aquifer. Mineral precipitation can occur at the discharging vents of the faults or in the subsurface.
- The hydraulic parameters of geological formations: enhanced lateral fluid migration within the upper aquifer occurred under the assigned hydraulic conductivities and porosities. The fluid flow can be maintained as long as these parameters are preserved and diagenetic mineral precipitation does not occur or, if precipitation does occur, secondary porosities and hydraulic conductivities are developed by burial diagenesis or related structural processes. During the simulations, the linear decrease in time of hydraulic conductivity within the upper aquifer resulted in reduced Darcy velocities. For low hydraulic conductivity formations in the system as granite (old Archaean crust, Nicholson granite and Barramundi basement) and basalt (Eastern Creek volcanics and Buddawadda basalt), basinal fluids circulate at insignificant velocities and cannot be regarded as a potential source for metal-

bearing fluids.

- Hydrothermal convection was achieved setting the stage for a possible mineralization event when the faults were represented as "active" by assigning higher hydraulic conductivities. The thermally driven convective circulation controlled the flow within the upper aquifer, where cold water recharging from the surface mixed with hotter upwelling brines. Free convection cells occurring in the upper diagenetic aquifer (within the sandstones and volcaniclastics of the Big Supersequence) likely formed during an early stage in the evolution of the Calvert Superbasin, when mineral precipitation did not decrease the permeability of the formation or seal the active faults. This process is in agreement with the previous findings of Bjorlykke et al. (1998) and Hewett (1986), who showed that rates of hydrothermal fluids flow controls diagenetic precipitation in clastic aquifers. As an overall observation through the various investigated cases and scenarios, convective flow cells allowed higher discharge temperatures and Darcy velocities at the vents of the active faults. However, discharge temperatures at the vents of the faults rarely exceeded 110-120^{0}C. For higher velocities along the faults (2-5 m/year), the Peclet number increases accordingly, until reaching a maximum value, after which when the discharge temperatures begin to drop, as a result of the convective heat flow becomes more important than the conductive transport. Garven (1985) reported a similar process.

Secondly, based on the modeling results, we tested the possibility of the accumulation of a SEDEX type ore deposit by mineral precipitation at the vents of the syn-sedimentary faults on the sea-floor or below the surface by examining the timing, origin, and temperature of hydrothermal outflow onto the sea floor, and comparing them to available mineralogical and geochemical data. Qualitatively favorable results were further investigated by estimating quantitatively the potential presence of such ore accumulations at the vents of the major faults F4 and F12. The results of this modeling effort could be used as a preliminary investigative technique before further detailed mineral exploration at a more local scale in the northern Lawn Hill Platform. The association of specific geological structures and hydrogeological conditions are of greatest interest, such as the presence of major faults, their depth of penetration, and the presence of suitable rocks that could act as either a source for metals leached by hydrothermal fluids (sandstones and conglomerates) or as traps for mineral precipitation (carbonates and siltstones).

Acknowledgments

This research was supported by the Natural Sciences and Engineering Research Council of Canada (NSERC) through a Discovery Grant (RGPIN 261283) and by the Canada Foundation for Innovation (CFI) through a New Opportunities Award to Jianwen Yang, University of Windsor, Ontario.

REFERENCES

Andrews, S.J. 1998. *Stratigraphy and depositional setting of the Upper McNamara Group, Lawn Hill Region, Northwest Queensland*, Economic Geology, **93**:1132 – 1152.

Betts P.G., Lister G.S. 2002. *Geodynamically indicated targeting strategy for shale- hosted massive sulfide Pb-Zn-Ag mineralisation in the Western Fold Belt, Mt Isa terrai*n, Australian Journal of Earth Sciences, **49**: 985.

Betts, P.G. 2000. *Asymmetric Extension of the lithosphere and its influence on Palaeoproterozoic Pb-Zn deposits of the Western Fold Belt, Mount Isa terrain. In: Lister, G.S. (ed.) Geological research for the exploration industry*, Journal of the Virtual Explorer, Electronic Edition, Volume 1, Paper 03. Available from http://virtualexplorer.com.au/2000/volume1/ailleres/ailleres.pdf

Bjorlykke, K., Mo, A., Palm, E. 1998. Modeling of thermal convection in sedimentary basins and its relevance to diagenetic reactions, Marine and Petroleum Geology, **5**, 338-51.

Blake D. H. 1987. *Geology of the Mount Isa Inlier and environs*, Queensland and Northern Territory Bulletin (Australia Bureau of Mineral Resources, Geology and Geophysics); 225. pp. 83.

Bradshaw, B.E.& Scott, D.L. 1999. *Integrated basin analysis of the Isa Superbasin using seismic, well-log and geopotential data: an evaluation of the economic potential of the Northern Lawn Hill Platform*, Australian Geological Survey Organisation Record 1999/19.

Broadbent, G.C., Myers, R.E., Wright, J.V. 1998, *Geology and origin of shale hosted Zn-Pb-Ag mineralization at the Century deposit, Northwest Queensland, Australia*, Economic Geology, **93**: 1264-1294.

Bull, S.W. 1998. *Sedimentology of the Palaeoproterozoic Barney Creek Formation in DDH BMR McArthur 2, southern McArthur Basin, Northern Territory*, Australian Journal of Earth Sciences, **45**: 21–31.

Carr, G.R., Sun, S-S., Page, R.W., Hinman, M. 1996. *Recent developments in the use of lead isotope model ages in Proterozoic terrains*, MIC '96, New Developments in Metallogenic Research: The McArthur-Mount Isa-Cloncurry Minerals Province: Extended abstracts, James Cook University of North Queensland Economic Geology Research Unit, Contribution **55**: 28 – 32.

Cooke, D.R., Bull, S.W., Large, R.R., Mcgoldrick, P.J. 2000. *The importance of oxidized brines for the formation of Australian Proterozoic stratiform sediment-hosted Pb-Zn (SEDEX) deposits*, Economic Geology, **95**: 1-18.

Damian, F., Damian, G., & Constantina, C., 2009. *The Subvolcanic Magmatic Rocks from the Nistru Zone (Gutîi Mountains)*, Carpathian Journal of Earth and Environmental Sciences, Vol. 4, No. 2, p. 101 - 122.

Diersch, H. J. 1992. *Interactive, graphics-based finite element simulation of groundwater contamination process*, Adv. Engineering Software, **15**, 1-13.

Diersch, H.J. 1993. *Computational aspects in developing an interactive 3D groundwater transport simulator using FEM and GIS*, International Conference on Groundwater Quality management (GQM 93), Tallinn, Estonia, 6-9 September 1993, IAHS publication No. 220, pp. 313-326.

Diersch, H.J. 2005. I*nteractive, graphics based finite-elements simulation system FEFLOW for modeling groundwater flow, contaminant mass and heat transport processes*, Release 5.2, Reference manual, WASY Ltd, Berlin.

Evans, D.G. & Raffensperger, J.P. 1992, *On the stream function for variable-density groundwater flow*, Water Resources Research, **28**: 2141-5.

Garven, G. & Freeze, R.A. 1984. T*heoretical analysis of the role of groundwater flow in the genesis of stratabound ore deposits*, 1. Mathematical and numerical model. II. Quantitative results. American Journal of Science, **293**, 497-568

Garven, G.1985. *The role of regional fluid flow in the genesis of the Pine Point deposit, Western Canada sedimentary basin*, Economic Geology, **80**, 307-324.

Garven, G. 1995a. *Continental scale groundwater flow and geologic processes*, Annual Reviews Earth and Planetary Science, **23**: 89-117.

Garven, G. 1995b. *Continental scale groundwater flow and geological processes*, Annual Review of Earth and Planetary Sciences, **23**: 9119-9144.

Gelhar, L.W., Welty, C., Rehfeld, K.R. 1992, *A critical review of data on field-scale dispersion in aquifers*, Water Resources, Res., **28**(7): 1955-1974.

Glickson, M., Golding, S.D., Southgate, P.N. 2006. *Thermal Evolution of the Ore-Hosting Isa Superbasin: Central and Northern Lawn Hill Platform*, Economic Geology **101**: 1211-1229.

Golding, S.D., Uysal, I.T., Glikson, M., Baublys, K.A., Southgate, P.N. 2006. *Timing and Chemistry of Fluid-Flow Events in the Lawn Hill Platform, Northern Australia*, Economic Geology, **101**:1231–1250.

Goodfellow, W.D., Lydon, J.W., Turner, R.J.W. 1993. *Geology and genesis of stratiform sediment-hosted (SEDEX) zinc-lead-silver sulfide deposits,* in **Kirkham, R.V., Sinclaire, W.D., Thorpe, R.I., and Duke, J.M**., eds., Mineral Deposit Modeling: Geological Association of Canada, Special paper, **40**, pp. 201-253.

Hewett, T.A. 1986. *Porosity and mineral alteration by fluid flow through a temperature field*, In: reservoir Characterization, eds Lake LW, Carroll HB Jr, pp. 83-140, Academic Press, Orlando.

Hiatt, E.E. & Kyser, T.K. 2000. *Links between Depositional and Diagenetic Processes in Basin Analysis: Porosity and Permeability Evolution in Sedimentary Rocks*, pp. 63-92 in Kyser, K., (ed.) Fluids and Basin Evolution, Mineralogical Association of Canada, Ottawa, Canada, pp. 262 .

Hiatt, E.E., Fayek, M., Kyser, T.K., Polito, P. 2001. *The importance of early quartz cementation events in the evolution of aquifer properties of ancient sandstones: isotopic evidence from ion probe analysis of sandstones from the McArthur, Athabasca, and Thelon basins*, GSA Abstracts with Programs Vol. 33, No. 6, pp. A74.

Hobbs, B.E., Ord, A., Archibald, N.J., Walsh, J.L., Zhang, Y., Brown, M., Zhao, Z. 2000. *Geodynamic modeling as an exploration tool*, Australian Institute of Mining and Metallurgy Proceedings of Annual Conference, After 2000-the future of mining, Sydney, April 10-12, 34-39, Geological Association of Canada Special paper **40**, pp. 201-253.

Idnurm M. 2000. *Towards a High Resolution Late Palaeoproterozoic - Earliest Mesoproterozoic apparent polar wander path for northern Australia*, Australian Journal of Earth Sciences, **47**: 405 429.

Jackson, M.J., Simpson, E.L., Eriksson, K.A. 1990. *Facies and sequence stratigraphic analysis in an intracratonic, thermal relaxation basin: the early Proterozoic, lower Quilalar Formation and Ballara Quartzite, Mount Isa, Australia*, Sedimentology, **37**: 1053-1078.

Jackson, M.J., Scott, D.L., Rawlings, D.J. 2000. *Stratigraphic framework for the Leichhardt and Calvert Superbasins: review and correlations of the pre-1700 Ma successions between Mt Isa and McArthur River*, Australian Journal of Earth Sciences, **47**: 381 – 403.

Koziy L. 2004. *Numerical Modelling of Coupled Fluid Flow and Heat Transport on Section P3, Northern Lawn Hill Platform, Mt Isa Basin*, AMIRA Project P552 Final Report (2004), pp. 543–581

Krassay, A.A., Bradshaw, B.E., Domagala, J., Jackson, M.J. 2000a. *Siliciclastic shoreline to growth-faulted, turbiditic sub-basins: the Proterozoic River Supersequence of the upper McNamara Group on the Lawn Hill Platform, northern Australia*, Australian Journal of Earth Sciences, **47**: 533 - 562.

Krassay, A.A., Domagala, J., Bradshaw, B.E., Southgate, P.N. 2000b. *Lowstand ramps, fans and deep-water Paleoproterozoic and Mesoproterozoic facies of the Lawn Hill Platform: the Term, Lawn, Wide and Doom Supersequences of the Isa Superbasin, northern Australia*, Australian Journal of Earth Sciences, **47**: 563 - 597.

Large, R.R., Bull, S.W., Cooke, D.R., Mcgoldrick, P. 1998. *A genetic model for the HYC deposit, Australia: based on regional sedimentology, geochemistry, and sulfide sediment relationships*, Economic Geology, **93**: 1345-1368.

Large, R.R., Bull, S.W., Mcgoldrick, P. 2000. *Lithogeochemical halos and geochemical vectors to stratiform sediment hosted Zn-Pb-Ag deposits. Part 2: HYC Deposit, McArthur River, Northern Territory*, Journal of Geochemical Exploration, **68**: 105-126.

Large, R.R., Bull, S.W., Winefield, P.R. 2001. *Carbon and oxygen isotope halo in carbonates related to the McArthur River (HYC) Zn-Pb-Ag deposit; implications for sedimentation, ore genesis and mineral exploration*, Economic Geology, **96**: 1567-1593.

Leaman, D.E. 1998. *Structure, contents and setting of Pb-Zn mineralisation in the McArthur Basin, northern Australia*, Australian Journal of Earth Sciences, **45**: 3-20.

Mcgoldrick P.J. & Large R.R. 1998. *Proterozoic stratiform sediment-hosted Zn-Pb-Ag deposits*, AGSO Journal of Geology and Geophysics, **17(4)**: 189-196.

Neacşu, A., Popescu, G., Constantinescu, B., Vasilescu, A. & Ceccato D., 2009. *The Geochemical Signature of Native Gold From Roşia Montană and Musariu Ore Deposits Metaliferi Mts. (Romania); Preliminary Data*, Carpathian Journal of Earth and Environmental Sciences, 2009, Vol. 4, No. 1, p. 49 - 59.

Neuman, S.P. 1990. *Universal scaling of hydraulic conductivities and dispersivities in geologic media*, Water Resources Res.v. 26, **8**: 1749-1758.

Page, R.W., Jackson, M.J., Krassay, A.A. 2000. *Constraining sequence stratigraphy in the north Australian Basins: SHRIMP U-Pb zircon geochronology between Mt Isa and McArthur River*, Australian Journal of Earth Sciences, **47**: 431 – 459.

Pittman, E.D. 1979. *Porosity, diagenesis and productive capability of sandstone reservoirs*, SCHOLLE, P.A. AND SCHLUGER, P.R., eds., Aspects of diagenesis: Society of Economic Paleontologists and Mineralogists Special Publication, **26**: 159 – 173.

Plotinskaya, O., Damian, F., Prokofiev, V., Kovalenker, V., Damian, G., 2009. *Tellurides Occurrences in the Baia Mare Region, Romania. Carpathian Journal of Earth and Environmental Sciences*, Vol. 4, No. 2, p. 89 - 100.

Polito P.A., Kyser T.K., Golding S.D., Southgate P.N. 2006a. Z*inc Deposits and Related Mineralization of the Burketown Mineral Field, Including the World-Class Century Deposit, Northern Australia: Fluid Inclusion and Stable Isotope Evidence for Basin Fluid Sources*, Economic Geology v101, **6**: 1251-1273.

Polito, P.A., Kyser, T.K., Southgate, P.N., Jackson, M.J. 2006b. *Sandstone Diagenesis in the Mount Isa Basin: An Isotopic and Fluid Inclusion Perspective in Relation to District-Wide Zn, Pb, and Cu Mineralization*, Economic Geology v101, **6**: 1159-1188.

Raffensperger, J.P. & Garven, G. 1995. *The formation of unconformity-type uranium ore deposits. 2. Coupled hydrochemical modelling*, American Journal of Science, **295**: 639-696.

Scott, D.L., Southgate, P.N., Krassay, A.A., Jackson, M.J. 2004. *Determining Basement Configuration, Basin Shape and Sediment Architecture in northern Australia at 1640 Ma and 1575 Ma, the times of fluid migration and Pb-Zn-Ag deposit formation*, AMIRA project P552 Final Report (2004), 430-496.

Shewchuk, J.R. 1996. *Triangle: Engineering a 2D Quality Mesh Generator and Delaunay Triangulator*, Applied Computational Geometry: Towards Geometric Engineering, volume 1148 of Lecture Notes in Computer Science, pp. 203-222.

Shewchuk, J.R. 2002. *Delaunay Refinement Algorithms for Triangular Mesh Generation*, Computational Geometry: Theory and Applications **22**(1-3):21-74.

Simms, M.A. & Garven, G. 2004, *Thermal convection in faulted, extensional sedimentary basins: theoretical results from finite-element modelling*, Geofluids 4, pp.109-130.

Solomon, M. & Heinrich, C.A. 1992. *Are high-heat producing granites essential to the origin of giant lead-zinc deposits at Mount Isa and Mac Arthur River, Australia*, Exploration and Mining Geology, **1**: 85-91.

Southgate, P.N. 2004. *Overview of the project 'fluid flow in the Mt Isa and McArthur Basins*, AMIRA Project P552 Final Report (2004), pp. 3–16.

Southgate, P.N., Bradshaw, B.E., Domagala, J., Jackson, M.J., Idnurm, M., Krassay, A.A., Page, R.W., Sami T.T., Scott, D.L., Lindsay, J.F., Mcconachie, B.A., Tarlowski, C. 2000a. *Chronostratigraphic basin framework for Palaeoproterozoic rocks (1730 - 1575 Ma) in northern Australia and implications for base-metal mineralisation*, Australian Journal of Earth Sciences, **47**: 461-483.

Southgate, P.N., Scott, D.L., Sami, T.T., Domagala, J., Jackson, M.J., James, N.P., Kyser, T. K. 2000b. *Basin shape and sediment architecture in the Gun Supersequence: a strike-slip model for Pb-Zn-Ag ore genesis at Mt Isa*, Australian Journal of Earth Sciences, **47**: 509 - 532.

Winefield P. 1999. *Late Palaeoproterozoic carbonates, southern McArthur Basin, Northern Territory*, Ph.D. Thesis, University of Tasmania.

Xu, M. & Eckstein, Y. 1995. *Use of weighted least-squares method in evaluation of the relationship between dispersivity and field scale*, Groundwater, **33** (6): 905-908.

Yang, J., Bull, S., Large, R. 2004a. *Numerical investigation of salinity in controlling ore- forming fluid transport in sedimentary basins: example of the HYC deposit, Northern Australia*, Mineralium

Deposita, **39**: 622-631.

Yang, J., Large, R., Bull, S. 2004b. *Factors controlling free thermal convection in faults in sedimentary basins: implications for the formation of zinc-lead mineral deposits*, Geofluids **4** (3): 237–247.

Yang, J., Large, R., Bull, S., Scott, D. 2006. *Basin-scale numerical modeling to test the role of buoyancy driven fluid flow and heat transport in the formation of stratiform Zn-Pb-Ag deposits in the northern Mt Isa basin*, Economic Geology, **101**: 1275-1292.

Zhang, Y., Sorjonen-Ward, P., Ord, A., Southgate, P.N. 2006. *Fluid Flow during Deformation Associated with Structural Closure of the Isa Superbasin at 1575 Ma in the Central and Northern Lawn Hill Platform, Northern Australia*, Economic Geology, **101**: 1293-1312.

WASY Gmbh 2005. Institute for Water Resources, Planning and Systems Research, Waltersdorfer Strasse 105, D-12526 Berlin-Bohnsdorf, Germany.

Wyborn, L.A. 1987. *The petrology and geochemistry of alteration assemblages in the Eastern Creek Volcanics, as a guide to copper and uranium mobility associated with regional metamorphism and deformation, Mount Isa, Queensland*, Geological Society, London, Special Publications, **33**: 425-434.

Received at: 16. 03. 2009
Revised at: 05. 01. 2010
Accepted for publication 26. 01. 2010
Published online at: 02. 02. 2010